Influence of dye dispersion on photoelectric conversion properties of dye-containing titania electrodes

Hiromasa Nishikiori[†,*], Rudi Agus Setiawan[†], Kyohei Miyashita,[†] Katsuya Teshima,[†] Tsuneo Fujii[‡]

[†]Department of Environmental Science and Technology, Faculty of Engineering, Shinshu University, 4-17-1 Wakasato, Nagano 380-8553, Japan

[‡]Nagano Prefectural Institute of Technology, 813-8 Shimonogo, Ueda, Nagano 386-1211, Japan

Corresponding author: Hiromasa Nishikiori

Tel: +81-26-269-5536

Fax: +81-26-269-5531

E-mail: nishiki@shinshu-u.ac.jp

Department of Environmental Science and Technology, Faculty of Engineering,

Shinshu University, Wakasato, Nagano 380-8553, Japan

Abstract

The dye-dispersing titania electrodes were prepared from the dye-containing titanium alkoxide sols by a room temperature sol−gel process and steam treatment at 110°C. The spectroscopic and photoelectric conversion properties of the electrodes were investigated in order to clarify the influences of the dye dispersion and the co-dispersion of the two dyes on the electron transfer process. The fluorescein and eosin Y molecules were dispersed into the titania as their monomers. The shapes of the photocurrent action spectra of the fluorescein and/or eosin Y-dispersing titania electrodes well corresponded to those of their absorption spectra because the excited electrons in the dyes were directly injected into the titania conduction band without any interaction between the dye molecules, such as energy transfer. This result indicated that the dye molecules were separately encapsulated in the pores between the titania nanoparticles and tightly adsorbed or bonded to the titania particle surface. The internal quantum efficiency of the photoelectric conversion was higher than that of the conventional dye-adsorbing titania electrodes in which the dye molecules were easily aggregated, thus deactivated by the energy transfer. The co-dispersion of the two dyes on the titania surface allowed to effectively extend the visible light region for the photoelectric conversion.

Keywords: photoelectric conversion, dye dispersion, fluorescein, eosin Y, titania, sol−gel method

1. Introduction

The studies of the photoinduced electron transfer and photoelectric conversion in dye−titania systems concerning dye-sensitized solar cells or related energy conversion devices have occurred over the past 20 years.[1−3] Many studies involved systems consisting of some titania particles and the dye molecules adsorbed on them The dye molecules were adsorbed on the surface of the relatively large aggregates of the crystalline titania particles rather than on the individual titania particles. A combination of some dyes, which can widen the absorption region, requires a new technology to improve the light-harvesting efficiency from each dye molecule without any deactivation by the energy or electron transfer.[4−11] The dye−titania interaction is very important for the electron injection process in the dye-sensitized solar cells.[12−23] The functional groups were induced in the sensitized dye molecules in order to form a strong bond between the dye chromophor and the titania surface.[16,17,22] Each molecule prefers to bond to the titania surface without dye stacking for the efficient electron injection and reducing the energy transfer. The effective dye−titania interaction is performed by the high dye dispersion into the titania. The sol−gel reaction using a titanium alkoxide sol containing the dye molecules easily allows formation of the dye-dispersing titania films, which are amorphous or nanocrystalline.[24−28] In such systems, the dye molecules can be highly dispersed on the surface of the individual titania nanoparticles without their aggregation. It was reported that the dye molecules were also

encapsulated in the small pores of the sol−gel silica matrices.[29−34]

Steam treatment at around 100°C promotes the sol−gel reaction and anatase titania particle formation.[35,36] We previously studied that the hydrothermal treatment of a dye-dispersing amorphous titania film remarkably improved the photoelectric conversion efficiency due not only to its crystallization but also the dye−titanium complex formation.[35−41] The dye molecules in such materials exhibit a more efficient absorption and electron injection because they are finely dispersed in the amorphous or nanosized crystalline matrices compared to the conventional dye-adsorbed materials.[37,39,40]

In this study, the dye-dispersing titania electrodes were prepared from the dye-containing titanium alkoxide sols by a room temperature sol−gel process and steam treatment at 110°C. We used two xanthene dyes, fluorescein and eosin Y, as the sensitizers (Scheme 1) because they have high molar extinction coefficients for harvesting light energy [42] and a high solubility into ethanol used as the solvent of the sol−gel systems. The co-dispersion of the two dyes on the titania surface can effectively prevent the dye aggregation and enhance the visible light response. The dye-adsorbing titania electrodes for the conventional dye-sensitized solar cells were also prepared for comparison. The spectroscopic and photoelectric conversion properties of the electrodes were investigated in order to clarify the influences of the dye dispersion and the co-dispersion of the two dyes on the electron transfer process.

2. Experimental

2. 1. Materials

Fluorescein, eosin Y, titanium tetraisopropoxide, ethanol, hydrochloric acid, nitric acid, diethylene glycol, iodine, lithium iodide, and sodium hydroxide (Wako, S or reagent grade) were used without further purification. Water was ion-exchanged and distilled. Glass plates coated with the transparent ITO electrode (AGC Fabritech) were soaked in hydrochloric acid (0.10 mol dm^{-3}) for 2h and then rinsed with water. The electrolyte for the photoelectric measurements consisted of a diethylene glycol solution of iodine (5.0×10^{-2} mol dm^{-3}) and lithium iodide (0.50 mol dm^{-3}).

2. 2. Sample preparation

The sol–gel reaction system was prepared by mixing 5.0 cm^3 of titanium tetraisopropoxide, 25.0 cm^3 of ethanol, 0.21 cm^3 of water, and 0.21 cm^3 of concentrated nitric acid as the catalyst of the sol–gel reaction and labeled SG-0. Fluorescein (F) and eosin Y (EY) were individually dissolved into SG-0 at concentrations of 1.0×10^{-3}–1.0×10^{-2} mol dm^{-3}. The systems containing 1.0×10^{-3}, 2.0×10^{-3}, 5.0×10^{-3}, and 1.0×10^{-2} mol dm^{-3} of fluorescein and eosin Y were labeled SG-F1, -F2, -F3, and -F4 and SG-EY1, - EY2, - EY3, and - EY4, respectively. The system containing 1.0×10^{-2} mol dm^{-3} of fluorescein and the same concentration of eosin Y was also prepared and labeled SG-F-EY. The dip-coated

thin films were prepared from the systems in which the sol–gel reaction proceeded for 1 day to prepare the electrodes.

In order to prepare the electrode samples coated with the crystalline titania, the glass plates with the ITO transparent electrode were dip-coated in the dye-free system (SG-0) and then heated at 500 ºC for 30 min. These electrodes were labeled E-0. Furthermore, the working electrodes were prepared in a way in which the E-0 was dip-coated with SG-F1, -F2, -F3, and -F4 and SG-EY1, - EY2, - EY3, and - EY4. The E-0 was also dip-coated with SG-F-EY. Water was heated at 110 ºC and these electrode samples were exposed to its steam of about 140 kPa for 120 min. The working electrodes prepared using SG-* were labeled WE-*.

The dye-adsorbing titania electrodes for the conventional dye-sensitized solar cells were also prepared in order to compare them to our original samples. The SG-0 was spread on the glass plates with the ITO transparent electrode and heated at 500 ºC for 30 min. The relatively thick titania layer was prepared in order to adsorb a greater amount of dyes, which was comparable to the dye-dispersing titania samples. These electrodes were immersed in 1.0×10^{-3}, 5.0×10^{-3}, and 1.0×10^{-2} mol dm^{-3} fluorescein ethanol solutions and the same concentrations of the eosin Y ethanol solutions for 24 h, and labeled WE-F1(ads), -F2(ads), and -F3(ads), and WE-EY1(ads), -EY2(ads), and -EY3(ads), respectively. The electrode

immersed in the mixture of the 1.0×10^{-2} mol dm^{-3} fluorescein ethanol solution and the same concentration of the eosin Y ethanol solution for 24 h was labeled WE-F-EY(ads).

2.3. Measurements

The UV-visible absorption spectra of the prepared electrode samples were observed using a spectrophotometer (Shimadzu UV-2500). The amounts of the dyes existing in the electrode samples were estimated from the absorption spectra of the dyes eluted by the 0.1 mol dm^{-3} sodium hydroxide aqueous solution. The iodine-based electrolyte was allowed to soak into the space between the electrode sample and the counter Pt electrode. Monochromatic light obtained from a fluorescence spectrophotometer (Shimazdu RF-5300) with a 150 W Xe short arc lamp (Ushio UXL-155) was irradiated on the electrodes for the spectroscopic measurements. During the light irradiation, the short circuit currents of the electrodes were measured by an electrometer (Keithley model 617). The intensity at each wavelength of the light source was obtained using a power meter (Molectron PM500A) in order to estimate the incident photon to current conversion efficiency (IPCE) and internal quantum efficiency, i.e., adsorbed photon to current conversion efficiency, of the electrode samples. The light intensity was confirmed to correlate with the results of the potassium ferrioxalate actinometry. The visible absorbance of the present electrode samples was lower than 1.0 which was sufficient to measure the number of absorbed photons in order to calculate the quantum efficiency.

3. Results and discussion

3.1. Morphology of the titania films

The XRD patterns of the fluorescein- and eosin Y-dispersing titania films were obtained as a function of the treatment time in a previous study.[39] An anatase-type crystal was produced in the film steam-treated for 20 min although no peak was found in the XRD pattern of the untreated amorphous gel films.[35,36,38−41] There was a slight difference between the XRD patterns of the fluorescein- and eosin Y-dispersing samples.[39] The size of the anatase crystallites of these electrodes was estimated from their full-width at half-maximum of the 25° peak using Sherrer's equation. They were ca. 5 nm for the fluorescein- and eosin Y-dispersing layers after the steam treatment for 120 min and much smaller than that of the crystalline titania foundation prepared by heating, i.e., ca. 18 nm.[38−41] The steam-treated films consisted of 10–20 nm particles based on the SEM images from a previous study.[35,40,41] The thickness of the dye-containing layer of the dye-dispersing titania electrodes was ca. 350 nm. The thickness of the titania layer of the conventional dye-adsorbing electrodes was ca. 2.1 μm.

3.2. Absorption and photocurrent properties of the dye-dispersing titania electrodes

Fig. 1 shows the absorption and photocurrent spectra of the fluorescein-dispersing titania electrodes. The accurate band gaps cannot be estimated due to the gradual absorption rises

around the band edges although the UV absorption spectra are not shown.[39] This is caused by the low crystallinity of the titania layer compared to normally heated titania. The spectra of the fluorescein-dispersing electrodes are located around 480 nm, ranging over a wavelength wider than that observed in solvents. This result indicates that the main fluorescein species were the neutral or anion form (at 450–480 nm) and some fluorescein molecules existed as the dianion form (at around 490 nm).[43] In addition, the band at a wavelength longer than around 500 nm indicates that a some number of fluorescein molecules formed the dianion-like species resulting from the strong interaction and a chelating linkage between the carboxyl group of the dye and the titanium species, [12,13,16–18,22,44] i.e., the fluorescein−titania complex, as denoted in our study.[38−41] Scheme 2 shows a schematic model of the complex between the dye and titania surface. The neutral and anion species were preferentially desorbed from the inside of the titania gel film into the water phase during the steam treatment because the species was weakly trapped in the pores of the gel. On the other hand, the stream treatment increased the number of fluorescein molecules interacting with the titanium species.[35−41] The absorption of fluorescein in the electrode increased with an increase in the dye concentration without any significant change in the spectral shape.

The IPCE values in the UV range slightly depended on the dye concentration because the interaction between the dye molecules and titania was not very strong or did not inhibit the crystallization of the titania or the electron transport in the titania layer. On the other hand,

the IPCE in the visible range exhibited a peak at 500 nm and increased with an increase in the dye concentration without any significant change in the spectral shape. The 500 nm peak was longer than the absorption peak at around 480 nm, because the longer wavelength species, the fluorescein−titania complex, significantly contributed to the photocurrent generation.[38−41]

Fig. 2 shows the absorption and photocurrent spectra of the eosin Y-dispersing titania electrodes. The absorption peak of the eosin Y-dispersing electrodes was located around 530 nm longer than that of the dianion species in water [45] due to the ionic interaction with the titania surface. It is expected that the interaction of eosin Y with titania is weaker than that of fluorescein based on its sharp spectral shape, especially on the longer wavelength side.[39]

The IPCE values in the UV range slightly depended on the dye concentration, whereas those in visible range increased with an increase in the dye concentration similar to the fluorescein-dispersing electrodes. The spectral peak position for the eosin Y-dispersing electrodes was 540 nm and the spectral shape was relatively sharp, similar to their absorption spectra. This is because the interaction of eosin Y with titania is weaker than that of fluorescein, and its complex formation is more difficult. The LUMO level of the dye is an important factor for the rate of injection into the titania conduction band. The IPCE values of the fluorescein-dispersing electrode were improved by the steam treatment more than that of the eosin Y-dispersing electrode although the LUMO level of eosin Y is more negative than that of fluorescein.[23] Fluorescein formed a greater amount of the chelate complex than

eosin Y due to its higher reactivity with the titanium species that depends on the nucleophilicity of its oxygen atoms of the carboxylate and carbonyl. The complex formation is expected to be more effective for the electron injection.

The carboxyl group of fluorescein was transformed into the carboxylate and formed a chelate complex with the titanium species during the steam treatment, while eosin Y was only the carboxylate form.[39] The proton dissociation constants, pK_a values, of the carboxyl groups of fluorescein and eosin Y are 4.45 and 3.75, respectively.[45] The carboxylate oxygen of fluorescein is more nucleophilic than that of eosin Y, thus making it easier to form the coordination complex with metal species. Additionally, the quinone-like carbonyl group of the xanthene ring also interacted with the titanium species. This type of complex formation strongly depends on the pK_a values of the hydroxyl group of the xanthene ring, which are 6.80 for fluorescein and 2.81 for eosin Y.[45]

Fig. 3 shows the relationships between the dye concentration and the IPCE values for the fluorescein- and eosin Y-individually dispersing titania electrodes. The IPCE was proportional to the dye concentration in both electrodes. The dye molecules were almost homogeneously dispersed in the titania films without forming their aggregates. Based on this result, the photoelectric conversion efficiency for fluorescein was regarded as about two-times higher than that for eosin Y, depending on the light absorption and electron injection efficiencies.

Fig. 4 shows the absorption and photocurrent spectra of the fluorescein- and eosin Y-dispersing electrodes and two-dye-codispersing titania electrodes. The absorption and IPCE spectra of the two-dye-codispersing electrode corresponded to the sum of those for each dye-dispersing electrode. Both dye molecules were almost homogeneously dispersed in the titania films without their interaction and directly induced the electron injection into the titania conduction band.

3.3. Absorption and photocurrent properties of the dye-adsorbing titania electrodes

The absorption and photocurrent of the conventional dye-adsorbing titania electrodes were observed for comparison with those of the dye-dispersing electrodes. Fig. 5 shows the absorption and IPCE spectra of the fluorescein-adsorbing titania electrodes. The broad absorption spectra indicated the existence of the neutral, anion, and dianion species of fluorescein.[43] On the other hand, the relative intensity of the longer wavelength band at around 500−550 nm was weaker than that of the dye-dispersing electrodes, indicating the weaker interaction with the titania. The absorbance and IPCE values increased with the dye content. The bands on the shorter wavelength side, around 400 nm, were due to the longer absorption edge of the titania with some amount of defects.[39] The values higher than those of the dye-dispersing electrodes are due to the much thicker titania layer. The peaks of the IPCE spectra were observed at 500 nm, similar to those of the fluorescein-dispersing electrodes, indicating that the fluorescein−titania complex significantly

contributed to the photocurrent generation.[38−41] However, IPCE values were not proportional to the absorbance because the dye molecules easily interacted with each other at the high concentration and were deactivated by energy or electron transfer. Such molecules weakly interacted with the titania and exhibited low electron injection efficiency in the systems.

Fig. 6 shows the absorption and IPCE spectra of the eosin Y-adsorbing titania electrodes. The absorption band due to the eosin Y dimer was observed at around 500 nm in addition to the band at 530 nm due to the monomer of the eosin Y dianion.[20,46] On the other hand, the IPCE spectra did not clearly exhibit the dimer band although the band became broader with an increase in the dye content. The IPCE value did not necessarily increase with the dye content. These results indicated that the dye aggregation on the titania surface prevented the electron injection into the titania conduction band.[10,47] However, some dimers contributed to the photocurrent generation based on the IPCE spectral shape.

Fig. 7 shows the absorption and photocurrent spectra of the fluorescein- and eosin Y-adsorbing and both dye-coadsorbing titania electrodes. The absorption spectrum of the fluorescein and eosin Y-coadsorbing electrode corresponded to the sum of each dye-adsorbing electrode. On the other hand, the IPCE spectra did not agree with their absorption spectra. The IPCE values in the fluorescein absorption region, 450−500 nm, were lower than the expected ones. This can be due to the energy transfer from the

fluorescein to eosin Y in addition to the deactivation in the dye aggregates. Such phenomena were also observed in the conventional dye-sensitized systems reported in a previous study.[48] This is due to the good energy transfer condition of the superposition of the fluorescence band of fluorescein and absorption band of eosin Y.

3.4. Dye dispersion in the titania electrodes

The internal quantum efficiency for the photoelectric conversion of each electrode was estimated as shown in Table 1. These values were calculated from the absorptions and photocurrents at 500 and 540 nm, which are the peak wavelengths for fluorescein and eosin Y, respectively. The amounts of substance and concentrations of the dyes in the dye-dispersing and dye-adsorbing titania electrodes are shown in Fig. S1. The concentrations were estimated from the absorption spectra of the eluted dyes and the surface area and thickness of the titania layer. The internal quantum efficiency slightly depended on the dye concentration in the dye-dispersing electrodes in both the fluorescein and eosin Y. The values for fluorescein and eosin Y were determined to be around 6% and 5%, respectively. On the other hand, the values for the dye-adsorbing electrodes decreased with an increase in the dye content. The deviation for the internal quantum efficiency of the dye-adsorbing electrodes was lower than that for the dye-dispersing electrodes because the preparation process of the dye-adsorbing electrodes did not contain the dye desorption, which occurred during the steam treatment used to prepare the dye-dispersing electrodes. The

values for the fluorescein and eosin Y-codispersing electrode reflected those for the individually dye-dispersing electrodes, whereas the value at 500 nm for fluorescein in the fluorescein and eosin Y-coadsorbing electrode was lower than that in the fluorescein-adsorbing electrode. This result indicated that the energy transfer from fluorescein to eosin Y was due to the aggregates of the two dyes formed on the titania surface. Scheme 3 shows a diagram of the difference in the dye dispersion between the dye-adsorbing titania and dye-dispersing titania. The dye molecules were adsorbed on the surface of the relatively large aggregates of the crystalline titania particles in the dye-adsorbing titania. This easily induced the strong interaction between the dye molecules. In the dye-dispersing electrodes, the dye molecules were highly dispersed on the surface of the individual nanocrystalline titania particles without their aggregation.[35−41] The dye molecules were separately encapsulated in the pores of the titania nanoparticles and tightly adsorbed or bonded to the titania particle surface. The excited electrons in the dyes were directly injected into the titania conduction band without interaction between the dye molecules, such as energy transfer.

4. Conclusions

The dye-dispersing titania electrodes were prepared from the dye-containing titanium alkoxide sols by a room temperature sol−gel process and steam treatment at 110°C.

Fluorescein and eosin Y were used as the sensitizers. The dye-adsorbing titania electrodes for the conventional dye-sensitized solar cells were also prepared in order to compare them with our original samples. The spectroscopic and photoelectric conversion properties of the electrodes were investigated in order to clarify the influences of the dye dispersion and the co-dispersion of the two dyes on the electron transfer process. The fluorescein and eosin Y molecules were dispersed into the titania as their monomers in the dye-dispersing electrodes. The shapes of the photocurrent action spectra of the fluorescein and/or eosin Y-dispersing titania electrodes corresponded well to those of their absorption spectra because the excited electrons in the dyes were directly injected into the titania conduction band without interaction between the dye molecules, such as energy transfer. This result indicated that the dye molecules were separately encapsulated in the pores of the titania nanoparticles and tightly adsorbed or bonded to the titania particle surface. The internal quantum efficiency of the photoelectric conversion was higher than that of the conventional dye-adsorbing titania electrodes in which the dye molecules were easily aggregated and produced the deactivating energy transfer. The co-dispersion of the two dyes on the titania surface allowed effective extension of the visible light region for photoelectric conversion.

Acknowledgements

This work was supported by JSPS KAKENHI Grant Number 24550153.

References

1 B. O'Regan and M. Grätzel, *Nature*, 1991, **353**, 737−740.

2 M. K. Nazeeruddin, A. Kay, I. Rodicio, R. Hamphry-Baker, E. Müeller, P. Liska, N. Vlachopoulos and M. Grätzel, *J. Am. Chem. Soc.*, 1993, **115**, 6382−6390.

3 M. Grätzel, *J. Photochem. Photobiol. C: Photochem. Rev.*, 2003, **4**, 145−153.

4 J. J. Cid, J. H. Yum, S. R. Jang, M. K. Nazeeruddin, E. Martínez-Ferrero, E. Palomares, J. Ko, M. Grätzel and T. Torres, *Angew. Chem. Int. Ed.*, 2007, **46**, 8358−8362.

5 C. Siegers, U. Würfel, M. Zistler, H. Gores, J. Hohl-Ebinger, A. Hinsch and R. Haag, *Chem. Phys. Chem.*, 2008, **9**, 793−798.

6 M. J. Griffith, A. J. Mozer, G. Tsekouras, Y. Dong, P. Wagner, K. Wagner, G. G. Wallace, S. Mori and D. L. Officer, *Appl. Phys. Lett.*, 2011, **98**, 163502.

7 M. D. Brown, P. Parkinson, T. Torres, H. Miura, L. M. Herz and H. J. Snaith, *J. Phys. Chem. C*, 2011, **115**, 23204−23208.

8 B. E. Hardin, A. Sellinger, T. Moehl, R. Humphry-Baker, J. E. Moser, P. Wang, S. M. Zakeeruddin, M. Grätzel and M. D. McGehee, *J. Am. Chem. Soc.*, 2011, **133**, 10662−10667.

9 M. Kimura, H. Nomoto, N. Masaki and S. Mori, *Angew. Chem. Int. Ed.*, 2012, **51**, 4371

−4374.

10 H. Ozawa, R. Shimizu and H. Arakawa, *RSC Adv.*, 2012, **2**, 3198−3200.

11 D. Colonna, V. Capogna, A. Lembo, T. M. Brown, A. Reale and A. D. Carlo, *Appl. Phys. Express*, 2012, **5**, 022303.

12 K. Murakoshi, G. Kano, Y. Wada, S. Yanagida, H. Miyazaki, M. Matsumoto and S. Murasawa, *J. Electroanal. Chem.*, 1995, **396**, 27−34.

13 K. Kalyanasundaram and M. Grätzel, *Coord. Chem. Rev.*, 1998, **177**, 347−414.

14 J. He, F. Chen, J. Zhao and H. Hidaka, *Colloids Surf. A: Physicochem. Eng. Aspects*, 1998, **142**, 49−57.

15 C. Wang, C. Liu, Y. Wang and T. Shen, *J. Colloid Interface Sci.*, 1998, **197**, 126−132.

16 M. Hilgendorff and V. Sundström, *J. Phys. Chem. B*, 1998, **102**, 10505−10514.

17 G. Ramakrishna and H. N. Ghosh, *J. Phys. Chem. B*, 2001, **105**, 7000−7008.

18 G. Benkö, M. Hilgendorff, A. P. Yartsev and V. Sundström, *J. Phys. Chem. B*, 2001, **105**, 967−974.

19 G. Benkö, B. Skårman, R. Wallenberg, A. Hagfeldt, V. Sundström and A. P. Yartsev, *J. Phys. Chem. B*, 2003, **107**, 1370−1375.

20 S. Pelet, M. Grätzel and J. E. Moser, *J. Phys. Chem. B*, 2003, **107**, 3215−3224.

21 G. Ramakrishna, A. Das and H. N. Ghosh, *Langmuir*, 2004, **20**, 1430−1435.

22 D. El Mekkawi and M. S. A. Abdel-Mottaleb, *Int. J. Photoenergy*, 2005, **7**, 95−101.

23 G. D. Sharma, P. Balraju, M. Kumar and M. S. Roy, *Mater. Sci. Eng. B*, 2009, **162**, 32−39.

24 H. Dislich, *Angew. Chem., Int. Ed. Engl.*, 1971, **10**, 363−370.

25 H. Dislich, *J. Non-Cryst. Solids*, 1983, **57**, 371−388.

26 C. J. Brinker and G. W. Scherer, *Sol–Gel Science: The Physics and Chemistry of Sol–Gel Processing*, Academic Press, San Diego, 1990.

27 C. J. Brinker, G. C. Frye, A. J. Hurd and C. S. Ashley, *Thin Solid Films*, 1991, **201**, 97−108.

28 C. J. Brinker, A. J. Hurd, G. C. Frye, P. R. Schunk and C. S. Ashley, *J. Ceram. Soc. Jpn.*, 1991, **99**, 862−877.

29 D. Avnir , D. Levy and R. Reisfeld, *J. Phys. Chem.*, 1984, **88**, 5956−5959.

30 R. Reisfeld, R. Zusman, Y. Cohen and M. Eyal, *Chem. Phys. Lett.* 1988, **147**, 142−147.

31 T. Fujii, A. Ishii and M. Anpo, *J. Photochem. Photobiol. A: Chem.*, 1990, 54, 231−237.

32 U. Narang, F. V. Bright and P. N. Prasad, *Appl. Spectrosc.*, 1993, **47**, 229, 229−234.

33 H. Nishikiori and T. Fujii, *J. Phys. Chem. B*, 1997, **101**, 3680−3687.

34 H. Nishikiori, N. Tanaka, Y. Minami, A. Katsuki and T. Fujii, *J. Photochem. Photobiol. A: Chem.*, 2010, **212**, 62−67.

35 H. Nishikiori, N. Tanaka, T. Kitsui and T. Fujii, *J. Photochem. Photobiol. A: Chem.*, 2006, **179**, 125−129.

36 T. Kitsui, H. Nishikiori, N Tanaka and. T. Fujii, *J. Photochem. Photobiol. A: Chem.*, 2006, **192**, 220−225.

37 H. Nishikiori, W. Qian, M. A. El-Sayed, N. Tanaka and T. Fujii, *J. Phys. Chem. C*, 2007, **111**, 9008−9011.

38 H. Nishikiori, Y. Uesugi, N. Tanaka and T. Fujii, *J. Photochem. Photobiol. A: Chem.*, 2009, **207**, 204−208.

39 H. Nishikiori, Y. Uesugi, S. Takami, R. A. Setiawan, T. Fujii, W. Qian and M. A. El-Sayed, *J. Phys. Chem. C*, 2011, **115**, 2880−2887.

40 H. Nishikiori, Y. Uesugi, R. A. Setiawan, T. Fujii, W. Qian and M. A. El-Sayed, *J. Phys. Chem. C*, 2012, **116**, 4848−4854.

41 H. Nishikiori, R. A. Setiawan, K. Miyamoto, G. Sukmono, Y. Uesugi, K. Teshima and T. Fujii, *RSC Adv.*, 2012, **2**, 4258−4267.

42 M. Maeda, *Laser dyes : properties of organic compounds for dye lasers*, Academic Press, Tokyo, 1984.

43 T. Fujii, A. Ishii, N. Takusagawa and M. Anpo, Res. Chem. Intermed., 1992, **17**, 1−14.

44 J. N. O'Shea, J. B. Taylor and E. F. Smith, *Surf. Sci.*, 2004, **548**, 317−323.

45 N. O. Mchedlov-Petrossyan and V. N. Kleshchevnikova, *J. Chem. Soc. Faraday Trans.*, 1994, **90**, 629−640.

46 K. K. Rohatgi and A. K. Mukhopadhyay, *J. Phys. Chem.*, 1972, **76**, 3970−3973.

47 A. C. Khazraji, S. Hotchandani, S. Das and P. V. Kamat, *J. Phys. Chem. B*, 1999, **103**, 4693−4700.

48 S. Min and G. Lu, *Int. J. Hydrogen Energy*, 2012, **37**, 10564−10574.

Table 1 Internal quantum efficiency of photocurrent in each electrode

Electrode	Quantum efficiency / %
Fluorescein	
WE-F1	6.5±1.1 (500 nm)
WE-F2	5.7±1.2 (500 nm)
WE-F3	5.8±1.0 (500 nm)
WE-F4	6.2±0.7 (500 nm)
WE-F1(ads)	4.3±0.4 (500 nm)
WE-F2(ads)	3.6±0.3 (500 nm)
WE-F3(ads)	3.2±0.2 (500 nm)
Eosin Y	
WE-EY1	4.5±1.3 (540 nm)
WE-EY2	4.6±1.1 (540 nm)
WE-EY3	5.0±0.9 (540 nm)
WE-EY4	5.7±0.9 (540 nm)
WE-EY1(ads)	5.1±0.4 (540 nm)
WE-EY2(ads)	4.5±0.3 (540 nm)
WE-EY3(ads)	4.1±0.2 (540 nm)
Mixture	
WE-F-EY	6.5±0.7 (500 nm)
	6.2±0.4 (540 nm)
WE-F-EY(ads)	3.0±0.3 (500 nm)
	4.1±0.3 (540 nm)

Figure captions

Figure 1 (a) Absorption and (b) photocurrent spectra of the fluorescein-dispersing titania electrodes prepared from the titania sol containing (1) 1.0×10^{-3}, (2) 2.0×10^{-3}, (3) 5.0×10^{-3}, and (4)1.0×10^{-2} mol dm^{-3} fluorescein.

Figure 2 (a) Absorption and (b) photocurrent spectra of the eosin Y-dispersing titania electrodes prepared from the titania sol containing (1) 1.0×10^{-3}, (2) 2.0×10^{-3}, (3) 5.0×10^{-3}, and (4)1.0×10^{-2} mol dm^{-3} eosin Y.

Figure 3 The relationships between the dye concentration in the material sols and the IPCE values for the fluorescein- and eosin Y-dispersing titania electrodes estimated at 500 and 540 nm, respectively.

Figure 4 (a) Absorption and (b) photocurrent spectra of the fluorescein- and eosin Y-dispersing electrodes and two-dye-codispersing titania electrodes.

Figure 5 (a) Absorption and (b) photocurrent spectra of the fluorescein-adsorbing titania electrodes using (1) 1.0×10^{-3}, (2) 5.0×10^{-3}, and (3) 1.0×10^{-2} mol dm^{-3} of fluorescein

solutions.

Figure 6 (a) Absorption and (b) photocurrent spectra of the eosin Y-adsorbing titania electrodes using (1) 1.0×10^{-3}, (2) 5.0×10^{-3}, and (3) 1.0×10^{-2} mol dm^{-3} eosin Y solutions.

Figure 7 (a) Absorption and (b) photocurrent spectra of the fluorescein- and eosin Y-adsorbing and both dye-coadsorbing titania electrodes.

Scheme 1 Molecular forms of fluorescein and eosin Y.

Scheme 2 A schematic model of the complex between the dye molecule and titania surface.

Scheme 3 Diagram of dye dispersion in dye-adsorbing titania and dye-dispersing titania.

Figure 1

(a)

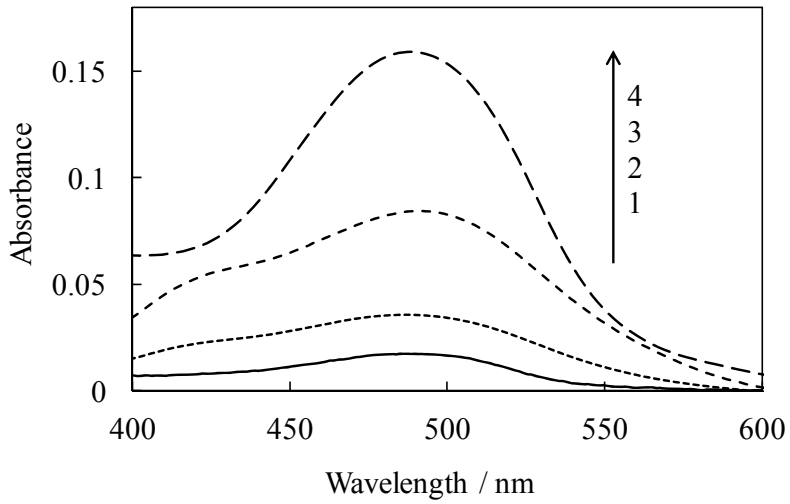
Absorbance
0.15
0.1
0.05
0
400
450
500
550
600
Wavelength / nm
4
3
2
1

(b)

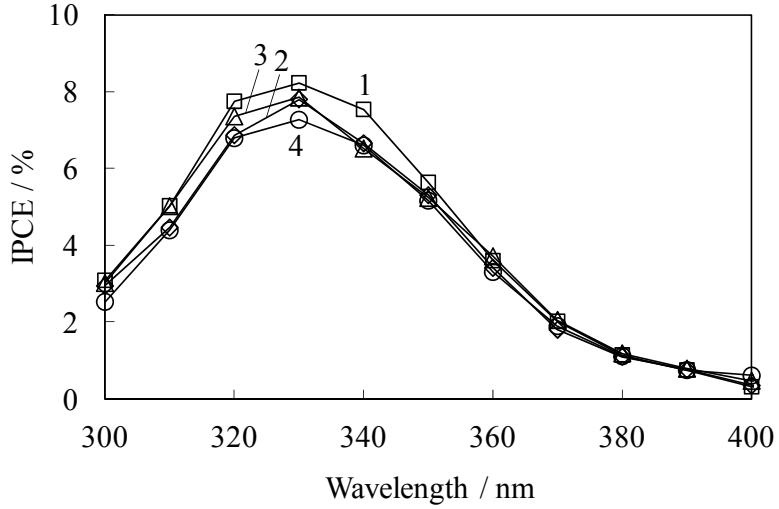
IPCE / %
10
8
6
4
2
0
300
320
340
360
380
400
Wavelength / nm
3
2
1
4

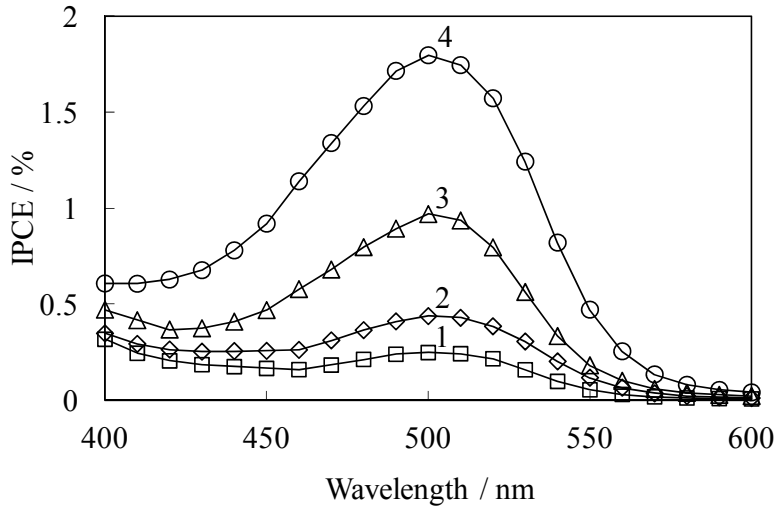
IPCE / %
2
1.5
1
0.5
0
400
450
500
550
600
Wavelength / nm
4
3
2
1

Figure 2

(a)

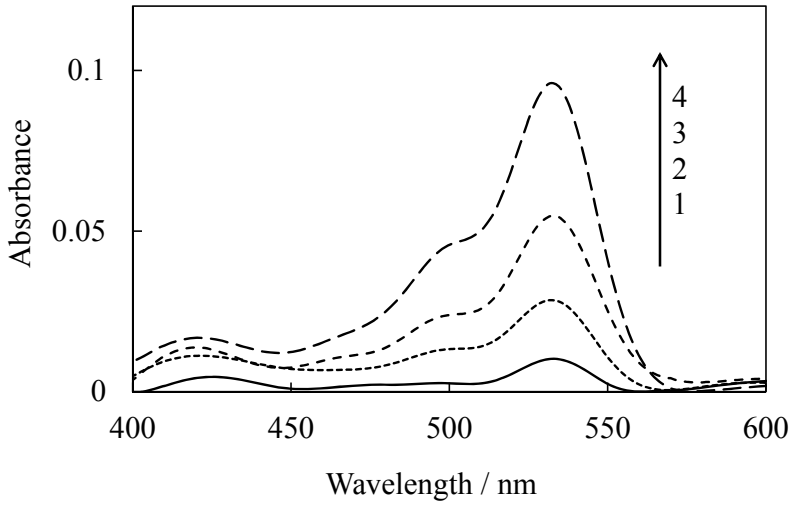
Absorbance
0.1
0.05
0
400
450
500
550
600
Wavelength / nm
4
3
2
1

(b)

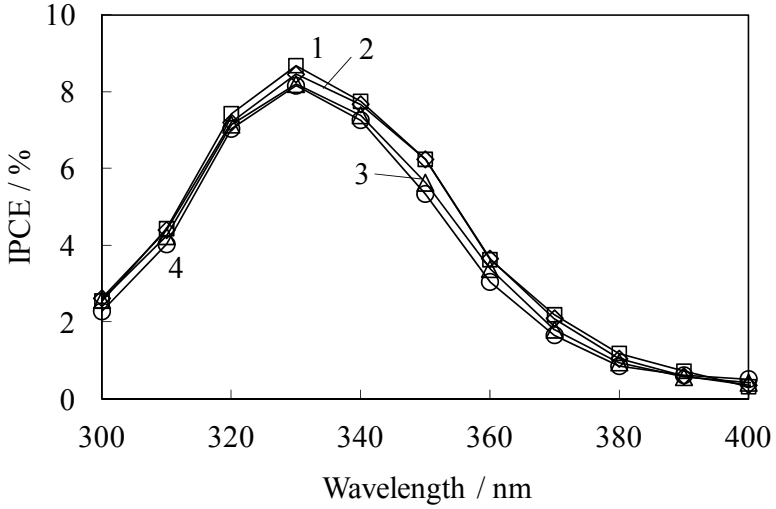
IPCE / %
10
8
6
4
2
0
300
320
340
360
380
400
Wavelength / nm
1
2
3
4

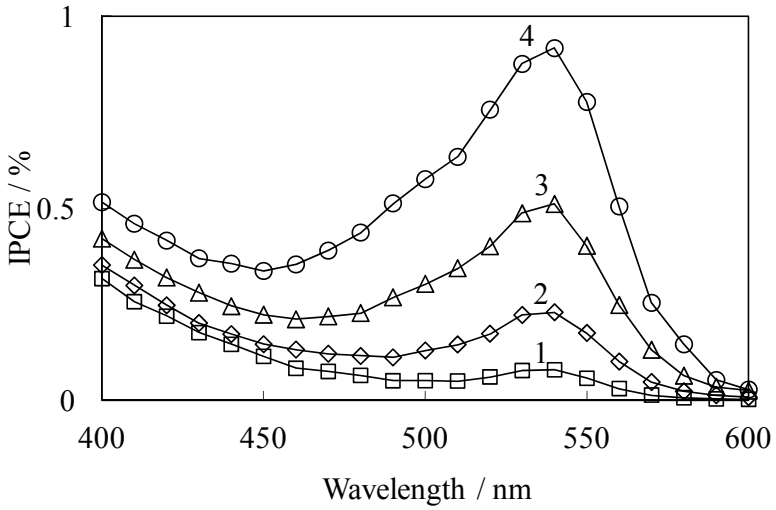
IPCE / %
1
0.5
0
400
450
500
550
600
Wavelength / nm
4
3
2
1

Figure 3

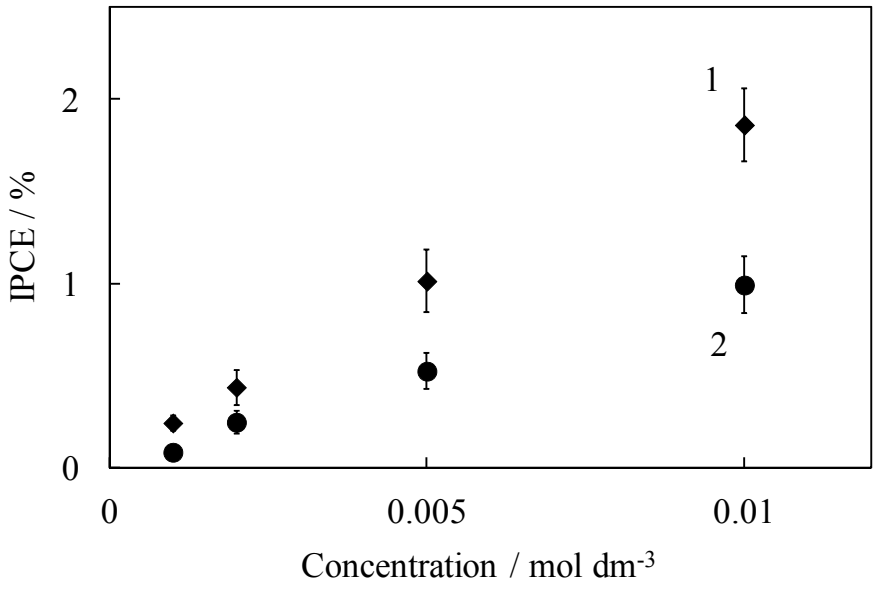

Figure 4

(a)

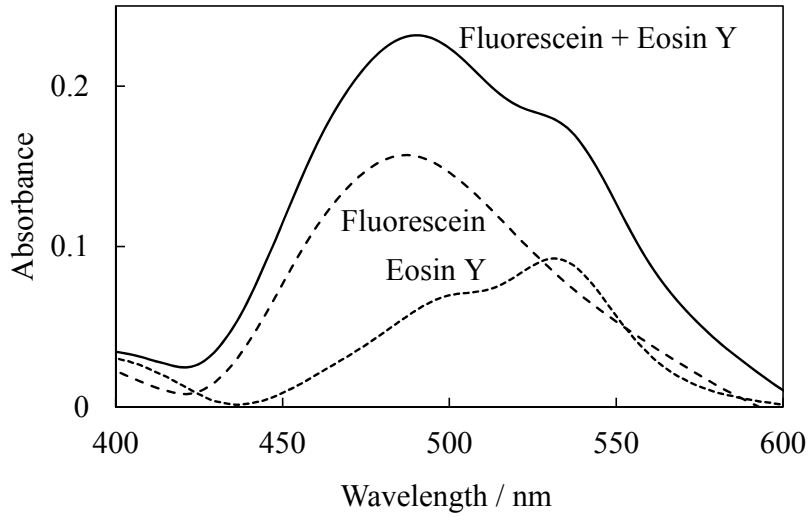
Fluorescein + Eosin Y
Fluorescein
Eosin Y
Absorbance
0
0.1
0.2
400
450
500
550
600
Wavelength / nm

(b)

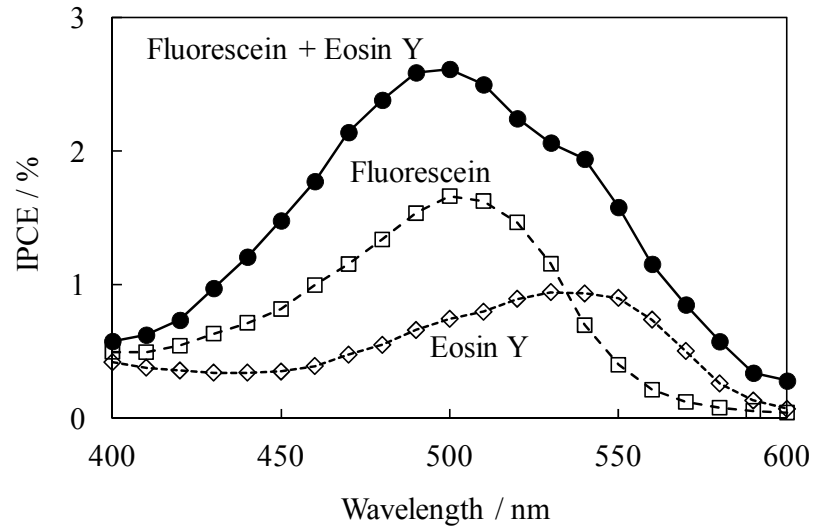
Fluorescein + Eosin Y
Fluorescein
Eosin Y
IPCE / %
0
1
2
3
400
450
500
550
600
Wavelength / nm

Figure 5

(a)

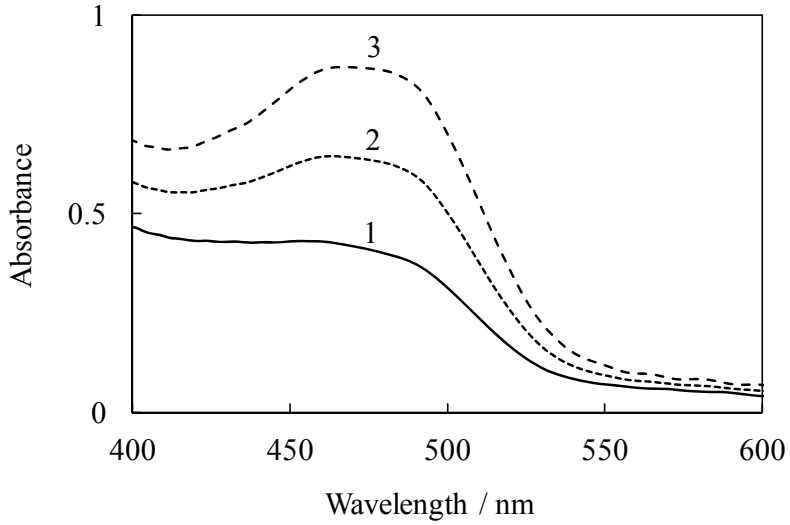
1
0.5
0
Absorbance
3
2
1
400
450
500
550
600
Wavelength / nm

(b)

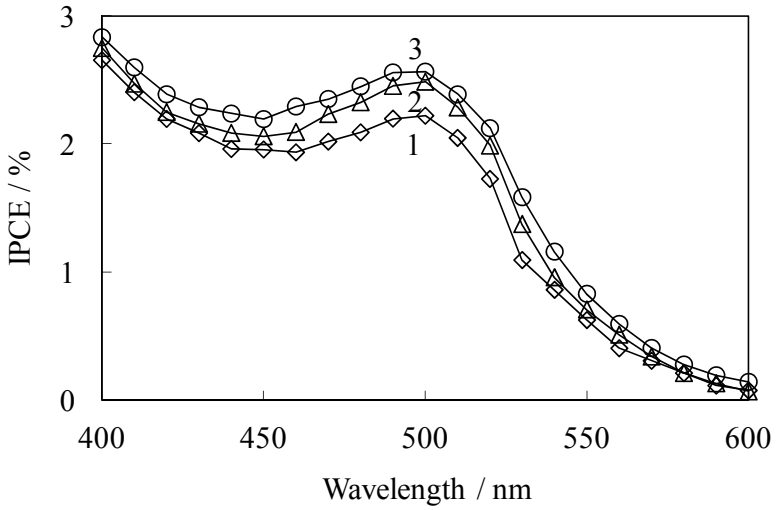
3
2
1
0
IPCE / %
3
2
1
400
450
500
550
600
Wavelength / nm

Figure 6

(a)

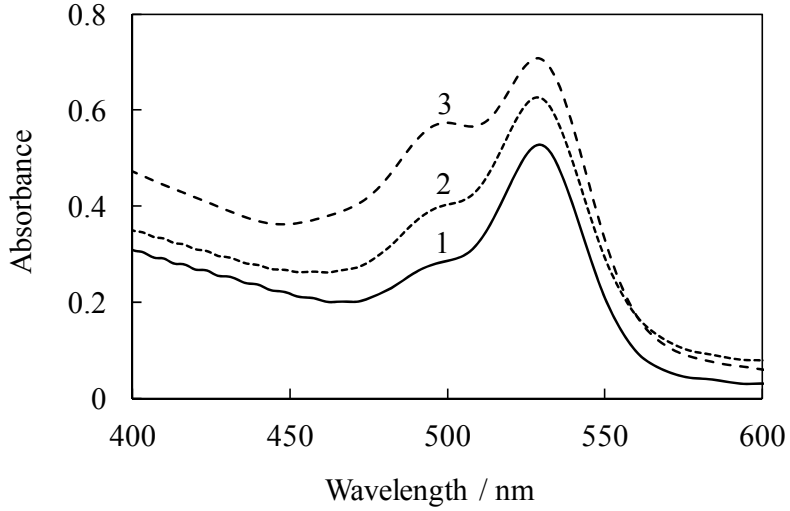
0.8
0.6
0.4
0.2
0
Absorbance
3
2
1
400
450
500
550
600
Wavelength / nm

(b)

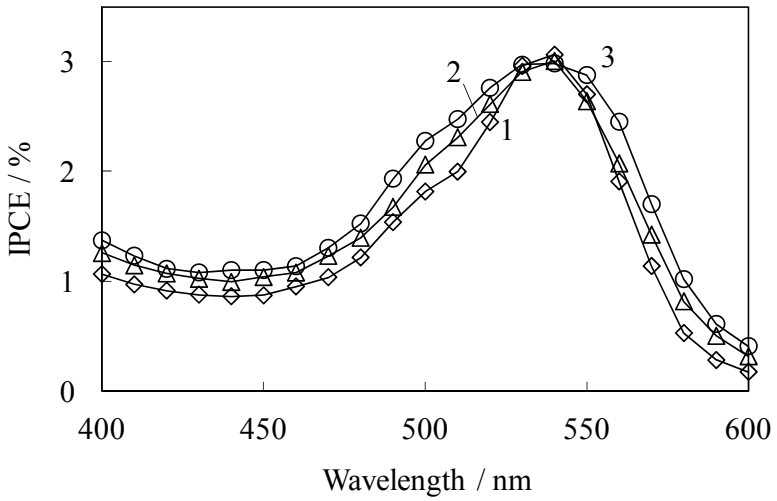
3
2
1
0
IPCE / %
2
3
1
400
450
500
550
600
Wavelength / nm

Figure 7

(a)

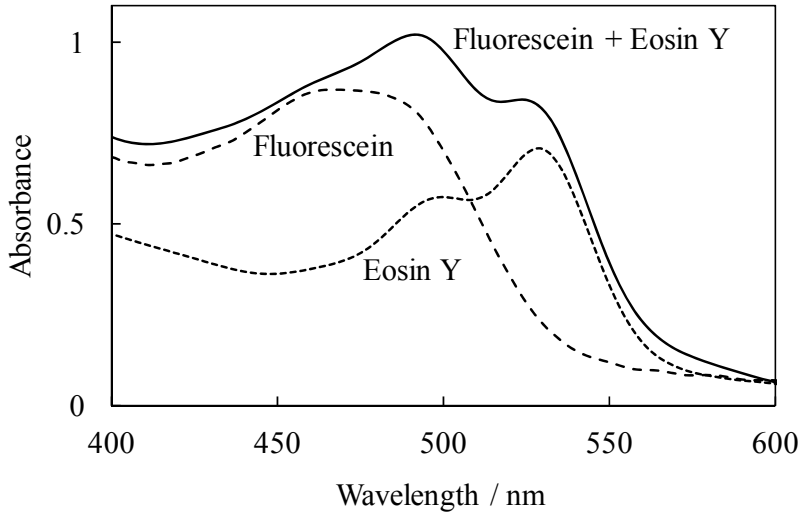
Fluorescein + Eosin Y
Fluorescein
Eosin Y
Absorbance
1
0.5
0
400
450
500
550
600
Wavelength / nm

(b)

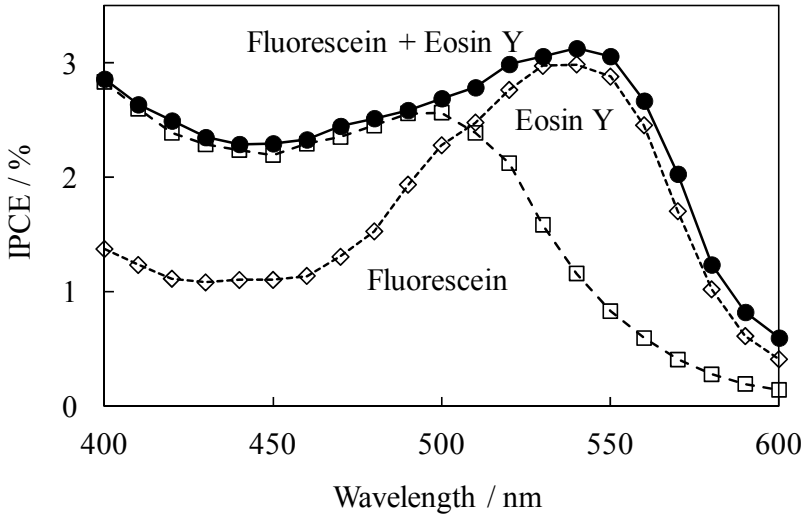
Fluorescein + Eosin Y
Eosin Y
Fluorescein
IPCE / %
3
2
1
0
400
450
500
550
600
Wavelength / nm

Scheme 1

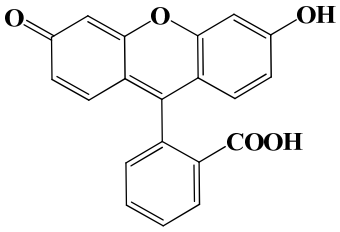

Fluorescein

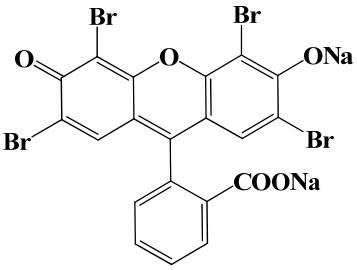

Eosin Y

Scheme 2

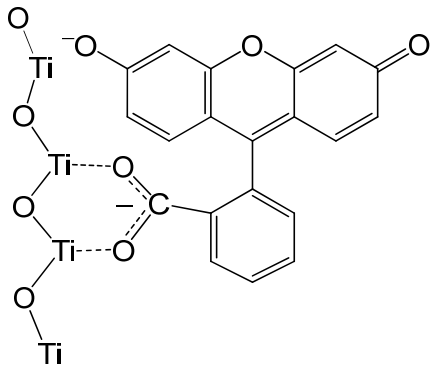

Scheme 3

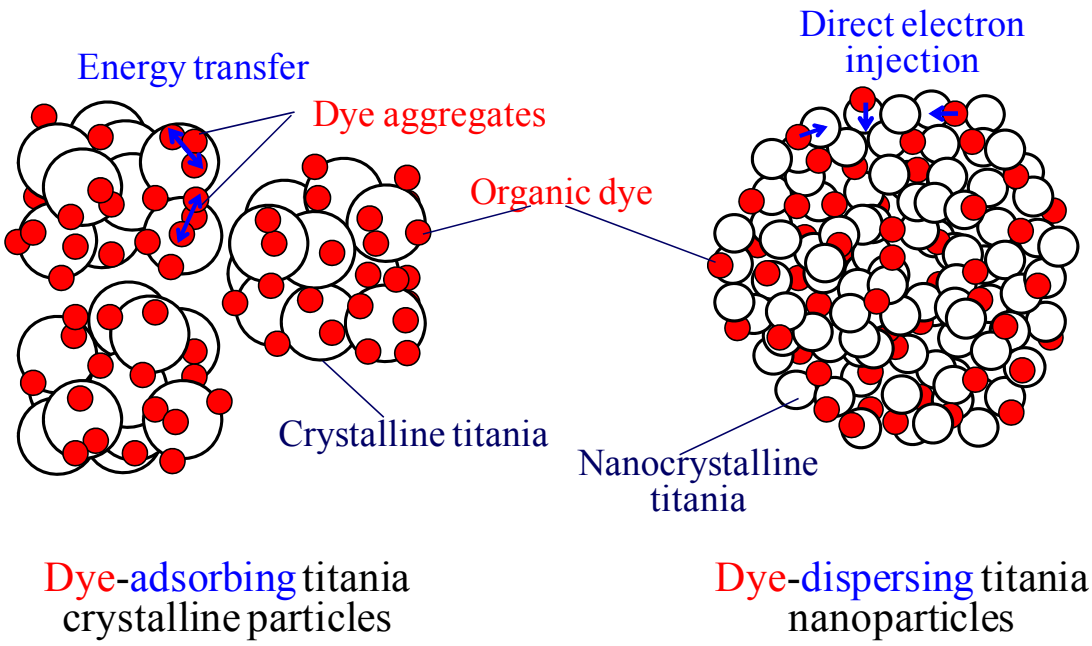
Energy transfer
Dye aggregates
Organic dye
Crystalline titania
Direct electron injection
Nanocrystalline titania
Dye-adsorbing titania crystalline particles
Dye-dispersing titania nanoparticles

Supplementary information

Figure S1

(a) Amounts of substance and (b) concentrations of fluorescein contained in the (1) dye-dispersing and (2) dye-adsorbing titania electrodes and eosin Y contained in the (3) dye-dispersing and (4) dye-adsorbing titania electrodes prepared from the systems containing each initial concentration of the dyes.

Figure S1

(a)

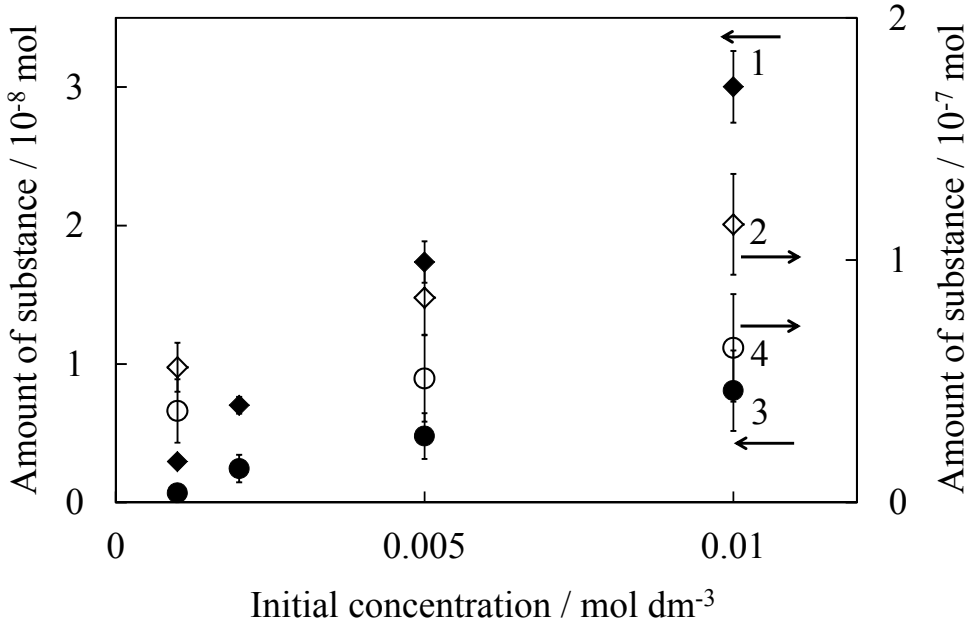
Amount of substance / 10-8 mol
Amount of substance / 10-7 mol
Initial concentration / mol dm-3
0
0.005
0.01
1
2
3
4

(b)

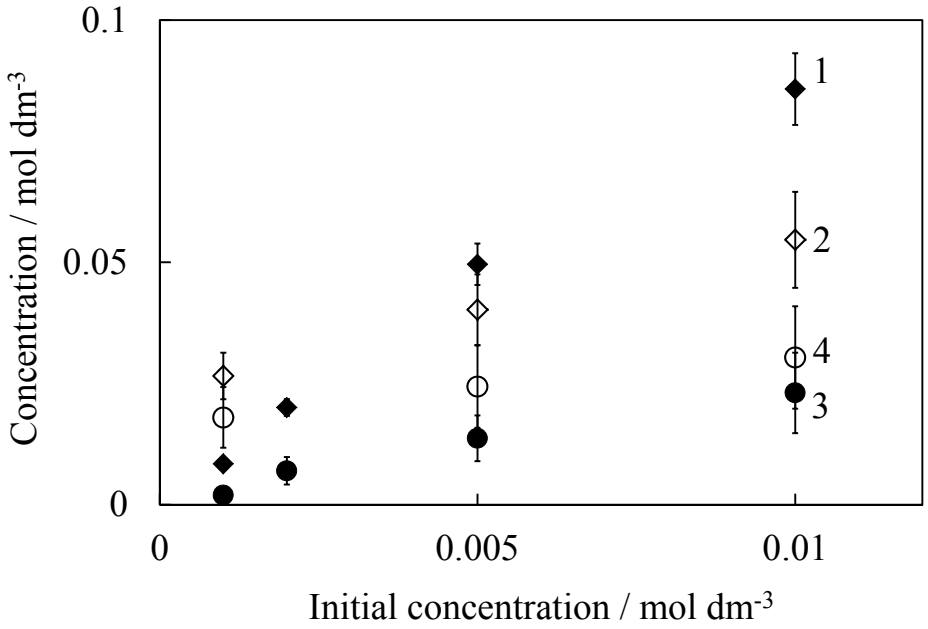
Concentration / mol dm-3
Initial concentration / mol dm-3
0
0.05
0.1
0.005
0.01
1
2
3
4